# Extractive Distillation with the Mixture of Ionic Liquid and Solid Inorganic Salt as Entrainers

**Zhigang Lei, Xiaomin Xi, Chengna Dai, Jiqin Zhu, and Biaohua Chen**
State Key Laboratory of Chemical Resource Engineering, Beijing University of Chemical Technology, Box 266, Beijing 100029 China

*DOI 10.1002/aic.14478*
*Published online May 9, 2014 in Wiley Online Library (wileyonlinelibrary.com)*

*The use of the mixture of ionic liquid (IL) and solid inorganic salt in place of the single IL as entrainers for extractive distillation, which integrates the advantages of a liquid solvent, that is, IL (easy operation and nonvolatility) and a solid salt (high separation ability) has been proposed in this work. The vapor–liquid equilibrium experiments indicated that the combination of $[EMIM]^+[Ac]^-$ and KAc is the most promising for the separation of ethanol and water among all of the entrainers investigated. Based on the thermodynamic study, the conceptual process design was developed to evaluate the competitiveness of the suggested entrainers for the separation of ethanol and water. It was determined that the overall heat duty on reboilers in the extractive distillation process using the new mixed entrainers decreases 19.04% compared with the benchmark entrainer $[EMIM]^+[Ac]^-$. Moreover, the density functional theory and COSMO-RS model were used to achieve theoretical insights at the molecular level.* © 2014 American Institute of Chemical Engineers
*AIChE J*, 60: 2994–3004, 2014
*Keywords: extractive distillation, ionic liquids, solid inorganic salts, mathematical model, theoretical analysis*

## Introduction

For the separation of azeotropic or close boiling mixtures, ordinary distillation processes cannot yield high purity components. In this case, extractive distillation, which combines the advantages of solvent extraction (high separation efficiency) and distillation (easy operation and high capacity), has been widely applied in industry. The selection of an efficient and suitable entrainer is the key to ensuring an economic operation. Currently, there are five types of entrainers used in extractive distillation, that is, solid salts,[1–4] liquid solvents,[5–8] the mixture of liquid solvents and solid salts,[9–12] hyperbranched polymers,[13] and ionic liquids (ILs).[13–29] Due to their unique advantages, such as nonvolatility, salt effect, high separation ability, regeneration, being present in the liquid state around room temperature, and thermal and chemical stabilities, ILs have received considerable attention in recent years for their use in extractive distillation for the separation of olefins and alkanes, alcohols and aliphatics, alcohols and water, and many other systems.[22–29] In principle, the salting effect of solid inorganic salts could be stronger than ILs due to their small molecular volumes.[30–32] However, when solid salt alone is used as an entrainer, dissolution, reuse, and transport of the solid salt are a significant problem in actual operation. Thus, in this work, a new type of physically mixed entrainers with the combination of IL and an inorganic salt were proposed aiming to obtain higher relative volatility (or selectivity) than using a single IL. It is known that extractive distillation is an energy-intensive process, and the use of an entrainer with a higher relative volatility (or selectivity) usually corresponds to a lower total annual cost.[33] Furthermore, both IL and solid salt are nonvolatile, rendering entrainer recovery by simple flash distillation or gas stripping feasible. In this sense, the mixed entrainers can still be taken on as environmentally friendly "green solvents."

To verify the applicability of the new type of entrainer (IL + inorganic salt) in extractive distillation, the separation of ethanol and water to produce high-purity ethanol was exemplified in this work. This is attributed to the following reasons: (a) the components form an azeotrope that cannot be separated by ordinary distillation; (b) this separation is the most studied process as a model system in the field of extractive distillation due to its important industrial value and the availability of both components; and (c) the new entrainers proposed in this work can also be applied to the separation of other aqueous solutions due to their similar separation mechanisms.

By far, all the IL entrainers used in extractive distillation for the separation of ethanol and water have been limited to single ILs. Calvar et al.[34–38] performed a systematic study on measuring the vapor–liquid equilibria (VLE) for the ternary systems of ethanol + water + IL (i.e., $[BMIM]^+[Cl]^-$, $[HMIM]^+[Cl]^-$, $[EMIM]^+[EtSO_4]^-$, $[BMIM]^+[MeSO_4]^-$, $[EMpy]^+[EtSO_4]^-$), showing that using the ILs at a specific mole fraction can break the existing azeotrope. Orchillés et al.[39,40] used $[EMIM]^+[TfO]^-$ and $[EMIM]^+[DCA]^-$ as entrainers to separate the ethanol and water mixtures. They claimed that $[EMIM]^+[DCA]^-$ could break the ethanol +

Additional Supporting Information may be found in the online version of this article.

Correspondence concerning this article should be addressed to Z. Lei at leizhg@mail.buct.edu.cn.

water azeotrope at a mole fraction of $x_{IL} = 0.019$, which was slightly smaller than that for $[EMIM]^+[TfO]^-$. Ge et al.[41] measured the isobaric VLE data of ethanol (1) + water (2) + IL (3) at different IL mass fractions, and the ethanol mole fraction was kept at 0.95 (IL-free). The results revealed that, among the eight ILs investigated, $[EMIM]^+[Ac]^-$ (breaking the ethanol and water azeotrope at $x_{IL} = 0.013$) had a significant effect on increasing the relative volatility of ethanol to water. Meanwhile, considering the melting point and its relatively low viscosity, $[EMIM]^+[Ac]^-$ might be a suitable candidate as an entrainer for industrial applications. Thus, in this work $[EMIM]^+[Ac]^-$ was chosen as the benchmark entrainer. It is noted that we refer to the IL $[EMIM]^+[Ac]^-$ rather than the volatile ethylene glycol as the benchmark entrainer because the former is now regarded as one of the most promising entrainers for the separation of ethanol and water.

This work is organized into four parts. First, the isobaric VLE experiments were performed to determine the optimum solid inorganic salt addition into IL as mixed entrainers for the separation of ethanol and water at the azeotropic composition. Second, to demonstrate the enhancement of the mixed entrainers with respect to pure IL on the separation performance, the isobaric VLE data over a full concentration range were measured for the ternary system of ethanol (1) + water (2) + $[EMIM]^+[Ac]^-$ (3) and the quaternary system of ethanol (1) + water (2) + $[EMIM]^+[Ac]^-$ (3) + optimum solid inorganic salt (4) at 101.3 kPa. Third, we tried to seek for some theoretical insights at the molecular level to explain why the addition of a little solid inorganic salt can enhance the separation performance by analyzing the binding energy, $\sigma$-profile, and the mixing enthalpy by means of density functional theory (DFT) and COSMO-RS models. Finally, the mathematical model for the conceptual process design using the new mixed entrainers was established using Aspen Plus software, into which the phase equilibrium model (NRTL) parameters obtained in this work were incorporated, to evaluate how much heat duty could be saved in the extractive distillation process using the suggested entrainer in comparison with the benchmark entrainer ($[EMIM]^+[Ac]^-$). Thus, this study ranges from the molecular level to industrial scale.

## Experimental Section

### *Materials*

Ethanol was purchased from Beijing J & K Scientific Ltd. with a purity above 99.9 wt %. Distilled water was degassed and filtered in the laboratory using a 0.2 μm Millipore filter to remove dust. The IL $[EMIM]^+[Ac]^-$ was purchased from Shanghai Cheng Jie Chemical Co. Ltd. with a purity above 99.0 wt %. The solid inorganic salts, that is, potassium acetate (KAc), potassium nitrate ($KNO_3$), potassium thiocyanate (KSCN), sodium acetate (NaAc), sodium bicarbonate ($NaHCO_3$), sodium nitrate ($NaNO_3$), and sodium thiocyanate (NaSCN) were purchased from Tianjin Guangfu Chemical Research Institute with purities above 98.0 wt %; and potassium chloride (KCl), potassium bicarbonate ($KHCO_3$), and sodium chloride (NaCl) were purchased from Beijing Chemical Works with purities above 98.5 wt %. Before the experiments, the IL was dried and degassed in a vacuum rotary evaporator at 333.2 K for 24 h to remove traces of water and other volatile impurities. The water content in IL was less than 400 ppm after pretreatment, as determined by Karl Fischer titration (SC-6) in our laboratory. The solid inorganic salts were dried in a DH-101 electric thermostat blast drying oven at 353.2 K for 2 h due to their hydroscopic nature.

### *Apparatus and procedure*

The VLE data were measured at atmospheric pressure by a circulation VLE still (a modified Othmer still). The details about this apparatus were described in our previous publications.[42–44] The compositions of ethanol and water in the liquid and vapor phases were detected by a gas chromatograph (GC 4000A) equipped with a TCD detector and a chromatographic column of Porapak-Q type (3 m × 3 mm). Data analysis was performed using an SC1100 workstation, and the compositions of the mixtures were calculated from the peak area of the samples.

The reliability of experimental data obtained in this work was verified beforehand by comparing the binary VLE data of ethanol (1) + water (2) at atmospheric pressure ($P = 101.3$ kPa) with those reported in the literatures.[39,45,46] The results are shown in Figure S1 (see Supporting Information), and the VLE data of ethanol (1) + water (2) is listed in Supporting Information Table S1. It can be seen from Supporting Information Figure S1 that the *x-y* curves almost overlap each other, verifying the reliability of the experimental apparatus. Furthermore, the experimental data were assessed through thermodynamic consistency by applying the Herington area test (see Supporting Information for more details).[47–49]

Similarly, isobaric VLE experiments were conducted to determine whether the mixtures of $[EMIM]^+[Ac]^-$ and solid inorganic salts as entrainers can improve the separation performance in comparison with single $[EMIM]^+[Ac]^-$ and to determine the optimum solid inorganic salt. On this basis, the isobaric VLE data at 101.3 kPa were measured for the ternary system of ethanol (1) + water (2) + $[EMIM]^+[Ac]^-$ (3), as well as the quaternary system of ethanol (1) + water (2) + $[EMIM]^+[Ac]^-$ (3) + solid inorganic salt (4), with respect to the optimum mixed entrainers. In this work, 10 solid inorganic salts were collected and tested. In the ternary and the quaternary systems, ethanol and water were at the azeotropic composition, and the mixed entrainers were kept at 10% mole fraction. In the quaternary system, the solid inorganic salt was kept at 5% mass fraction in the mixed entrainers. Because the amount of inorganic salt added to the IL is small, the effect of fusion heat can be ignored in this work.

## Computational Details

### *Quantum chemical calculations*

*DFT Calculations.* The binding energy reflects the degree of interaction between molecules and can be defined as the energy difference between a real system and an ideal system, for which the interaction between molecules is neglected and the physical properties are the same as the sum of all isolated molecules contained in the system. The binding energy between molecules A and B ($\Delta E_{A-B}$) can be calculated by

$$\Delta E_{A\text{-}B} = E(A+B) - E(A) - E(B) \quad (1)$$

where $\Delta E_{A-B}$ is the binding energy of the binary system; and $E(A)$, $E(B)$, and $E(A + B)$ are the sum of the electronic

and zero-point energies for single molecules A, B, and the mixture of A and B, respectively.

To obtain the binding energy between water (or ethanol) and the entrainers, all optimized geometries were obtained by using the Gaussian 03 software package[50] at the M05-2X/6-311++G(d,p) level with the keyword "int = ultrafine," which has been previously used for studying the interactions between ILs and polar organic molecules.[51,52] The M05-2X functional is one of the newest DFT methods and is assumed to correctly reproduce weak interactions.[53] To obtain the most favorable clusters (composed of IL ions, KAc, water, and ethanol), harmonic frequency analysis calculations were performed to verify the optimized geometries to obtain the lowest energy points (no imaginary frequency) rather than local minima. In addition to finding the optimized geometries, different initial structures were considered in this work, as shown in Supporting Information, where the total electronic energies and Cartesian coordinates of all these optimized structures are also given.

*COSMO-RS Calculations.* The COSMO-RS model, using a statistical thermodynamics approach based on the results of quantum chemical calculations, is a prior predicted thermodynamic method for fluid equilibrium and an efficient variant of dielectric continuum solvation methods.[54–61] The polarization charge densities ($\sigma$-profiles) for ethanol, water, cations, and anions ($[EMIM]^+$, $K^+$, $Na^+$, $NO_3^-$, $Cl^-$, $HCO_3^-$, $SCN^-$, and $Ac^-$) and the excess enthalpies of water (1) + entrainer (2) and ethanol (1) + entrainer (2) systems were analyzed using the COSMOthermX package to provide some theoretical insight for the separation of ethanol and water at the molecular level. To compute the thermodynamic properties of the pure components or mixtures, the optimized geometries should be first introduced into the COSMOthermX package. In this work, the geometries of ethanol and water were taken from the TZVP-C30–1301 databank, whereas the others were optimized at the BP86/TZVP computational level in the ideal gas phase using the Gaussian 03 package, as aforementioned.

### *VLE model (NRTL model)*

Because the NRTL model (see Supporting Information for model details) is the most common for correlating the VLE data of systems containing ILs,[45,58–66] this model was adopted in this work. The following minimized objective function was used to correlate the binary interaction parameters ($\Delta g_{ij}$ and $\Delta g_{ji}$)

$$\text{OF}\ (\%) = \frac{1}{N}\sum_{i=1}^{N}\left|\frac{\gamma_i^{\text{exp}} - \gamma_i^{\text{cal}}}{\gamma_i^{\text{exp}}}\right| \times 100 \tag{2}$$

where $N$ is the number of data points. The Marquardt method, as in Press et al.[67], which was programmed with the Visual Basic language, was used to fit the model parameters $\Delta g_{ij}$ and $\Delta g_{ji}$. $\gamma_i^{\text{exp}}$ and $\gamma_i^{\text{cal}}$ are the experimental and calculated activity coefficients of component $i$, respectively.

In the NRTL model, the nonrandomness parameter for the ethanol (1) + water (2) system is set to 0.40, and the corresponding binary interaction parameters $\Delta g_{12}$ and $\Delta g_{21}$ come from the literature.[68] The nonrandomness parameters for the ethanol (1) + water (2) + $[EMIM]^+[Ac]^-$ (3) + KAc (4) system, that is, $\alpha_{13}$, $\alpha_{14}$, $\alpha_{23}$, $\alpha_{24}$, and $\alpha_{34}$, are set to 0.30, 0.30, 0.30, 0.30, and 0.47, respectively. The binary interaction parameters ($\Delta g_{ij}$ and $\Delta g_{ji}$) between ethanol (or water) and IL were first correlated from the VLE data of the ethanol (1) + water (2) + $[EMIM]^+[Ac]^-$ (3) ternary system. Then, these values were used in conjunction with the VLE data of the ethanol (1) + water (2) + $[EMIM]^+[Ac]^-$ (3) + KAc (4) quaternary system to obtain the binary interaction parameters between ethanol (or water, or $[EMIM]^+[Ac]^-$) and KAc.

### *Process simulation calculations*

The extractive distillation process using the mixture of $[EMIM]^+[Ac]^-$ and KAc as entrainers was compared with that using the single $[EMIM]^+[Ac]^-$. The process simulation was performed by Aspen Plus software (version 7.1), in which the rigorous equilibrium (EQ) stage model RadFrac was established. In the process simulation, ethanol, water, and KAc were selected as conventional compounds from the databank of Aspen Plus software. The IL was defined as a new compound by the UNIFAC group method, and the physical properties, such as density, specific heat capacity, and critical properties, were estimated by group contribution methods.[69–71] Although it has been proved that COSMO-based methodologies are capable of the estimations of IL physical properties,[72–78] the group contribution methods based on experimental data are more accurate than the COSMO-based methodologies in most cases.

Recently, it was reported that COSMO-based property models can be implemented by default into Aspen Plus or Aspen HYSYS process simulations.[79–81] The integration of the COSMOSAC model into Aspen Plus was a good strategy for studying the processes of reuterin purification and toluene absorption. Moreover, it was found that the model can adequately and reasonably describe the properties and VLE data for these systems.[79,81] However, the COSMO-based methods still exhibit some theoretical and practical limitations for predicting the VLE data for the mixture of ethanol and water when using neither the TZVP basis set nor using the FINE-TZVP set, although the description of specific H-bond interactions is improved. Considering the strong polar systems investigated in this work, the NRTL model instead of the COSMOSAC property model was adopted in this work to obtain more realistic and accurate results. Furthermore, the NRTL model has a much higher accuracy for describing the VLE of the investigated systems, and the comparison between the experimental VLE data and the calculated results by the COSMO-RS and NRTL models is shown in Figures S3 to S5 in Supporting Information.

## Results and Discussion

### *Screening of the mixtures of IL and solid inorganic salts*

The activity coefficient of component $i$ ($\gamma_i$), which reflects the effect of the entrainer on the solution nonideality, can be calculated by the following equation

$$\gamma_i = \frac{y_i P}{x_i P_i^s} \tag{3}$$

where $y_i$ is the mole fraction of component $i$ in the equilibrium vapor phase; $x_i$ is mole fraction of component $i$ in the liquid phase containing entrainer; $P$ is the total pressure of the system, which equals to 101.3 kPa in this work; and $P_i^s$ is the vapor pressure of pure component $i$ at the equilibrium temperature as obtained by the Antoine equation using the

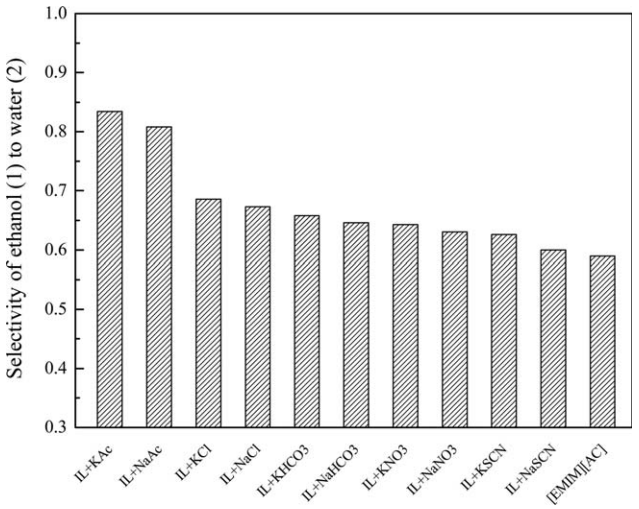


**Figure 1. Selectivity of ethanol (1) to water (2) at finite concentration with various mixed entrainers at 298.2 K.**

**Ethanol and water are at the azeotropic composition, and the mixed entrainer, in which the solid inorganic salt was kept at 5% mass fraction, was kept at 10% mole fraction in the solution.**

Antoine coefficients from the literature,[82] as listed in Table S2 in Supporting Information.

The isobaric VLE data at atmospheric pressure ($P = 101.3$ kPa) for the quaternary system of ethanol (1) + water (2) + $[EMIM]^+[Ac]^-$ (3) + solid inorganic salt (4) were measured. The detailed experimental data containing the equilibrium temperature ($T$), mole fraction of ethanol in the liquid phase ($x_1$) based on a salt-free basis in the vapor phase ($y_1$), activity coefficients of ethanol ($\gamma_1$) and water ($\gamma_2$), and the selectivity of ethanol to water ($S_{12}$) are listed in Table S3 (Supporting Information).

The experimental results are shown in Figure 1, from which we can see that all the mixed entrainers investigated improve the selectivity of ethanol to water in comparison with the single $[EMIM]^+[Ac]^-$, and KAc is the optimum solid inorganic salt among all the solid inorganic salts investigated. Thus, $[EMIM]^+[Ac]^-$ plus KAc will be selected as the mixed entrainers in subsequent studies.

### *VLE experiment over a full concentration rage*

The relative volatility ($\alpha_{12}$) of ethanol (1) to water (2) is calculated by

$$\alpha_{12} = \frac{y_1/x_1}{y_2/x_2} \tag{4}$$

The VLE experimental data of the ternary system of ethanol (1) + water (2) + $[EMIM]^+[Ac]^-$ (3) and the quaternary system of ethanol (1) + water (2) + $[EMIM]^+[Ac]^-$ (3) + KAc (4) are listed in Table S4 to Table S7 in the Supporting Information.

The $x_1'$-$y_1$ and $x_1'$-$\alpha_{12}$ curves with the mixed entrainers $[EMIM]^+[Ac]^-$ (3) + KAc (4) with respect to the benchmarked solvent $[EMIM]^+[Ac]^-$ at a full concentration range are shown in Figure 2. It is obvious that the addition of KAc to the IL entrainer improves the salting-out effect of $[EMIM]^+[Ac]^-$ and enhances the ethanol/water separation. Moreover, the higher the concentration of KAc in the mixed entrainers is, the higher the relative volatility of ethanol to water at the same concentration as the single IL. This result is not surprising because the smaller cation volume paired with the same anion is more effective for improving the relative volatility of the components to be separated. However, we would not expect a high salt concentration due to the solubility constraint in the solution.

### *Theoretical insights at the molecular level*

In this work, we tried to explain the reason why the addition of a small amount of solid inorganic salt into IL can significantly improve the separation performance, providing some theoretical insight at the molecular level. In this regard, the DFT and COSMO-RS model are useful theoretical tools.

*Effect of the Binding Energy.* The geometric structures optimized by Gaussian 03 are shown in Figure 3, and the corresponding binding energies between the entrainer and water (or ethanol) calculated by quantum chemistry calculations are listed in Table 1.

The binding energy between ethanol and water is $-30.8$ kJ $mol^{-1}$, whereas the binding energies between water molecules and KAc, $[EMIM]^+[Ac]^-$ and the mixture of $[EMIM]^+[Ac]^-$ and KAc are $-77.0$, $-62.1$, and $-67.4$ kJ $mol^{-1}$, respectively, indicating a stronger interaction between water and the new entrainers than between water and ethanol. The strong interaction between water and the new entrainer weakens the ethanol–water interaction, thus increasing the relative volatility of ethanol to water.

*Analysis of the σ-Profiles for Ethanol, Water, and Different Ions.* The thermodynamic properties of liquid and fluid mixtures with respect to the molecular surface charge density of their individual compounds can be derived from quantum chemical calculations using the COSMO-RS model.[83,84] The $\sigma$-profile is used to characterize the local polarity of the molecular surface and determine whether the hydrogen bond interaction between different molecules is strong or not.[85] The $\sigma$-profiles for water, ethanol, cations ($K^+$, $Na^+$, and $[EMIM]^+$), and anions ($Ac^-$, $HCO_3^-$, $Cl^-$, $NO_3^-$, and $SCN^-$) are illustrated in Figure 4, in which the two vertical dashed lines denote the cutoff radius for the hydrogen bond donor ($\sigma < -0.0082$ e/Å$^2$) and acceptor ($\sigma > 0.0082$ e/Å$^2$).[85,86] The range of $-0.0082$ e/Å$^2 < \sigma < 0.0082$ e/Å$^2$ is determined as nonpolar surface regions (mainly corresponding to —CH and —$CH_2$ groups). If the value of $\sigma$ for a molecule or segment is smaller than $-0.0082$ e/Å$^2$, the molecule or segment would have hydrogen bond donator ability. Otherwise, it would have acceptor ability if $\sigma > 0.0082$ e/Å$^2$.

Some peaks of water molecules are located in the left zone, and the polarization charge density $\sigma$ approximates $-0.02$ e/Å$^2$, indicating that water has a very strong hydrogen bond donator ability (protons of –OH). Meanwhile, the water molecule also has peaks at the $\sigma > 0.0082$ e/Å$^2$ zone, indicating that the oxygen atom of the water molecule has a strong hydrogen bond acceptor ability. This explains the formation of the strong hydrogen bonds between water molecules. $Ethanol_1$ and $ethanol_2$ are the isomers of the ethanol molecule, and the small difference between the isomers in their stable structures and lowest energy leads to the slightly different $\sigma$-profiles.[85,87] The main peaks of ethanol molecule lie in the nonpolar surface regions. Nevertheless, a small part lies in the left zone ($\sigma < -0.0082$ e/Å$^2$) and right zone ($\sigma > 0.0082$ e/Å$^2$), indicating that ethanol molecule has only

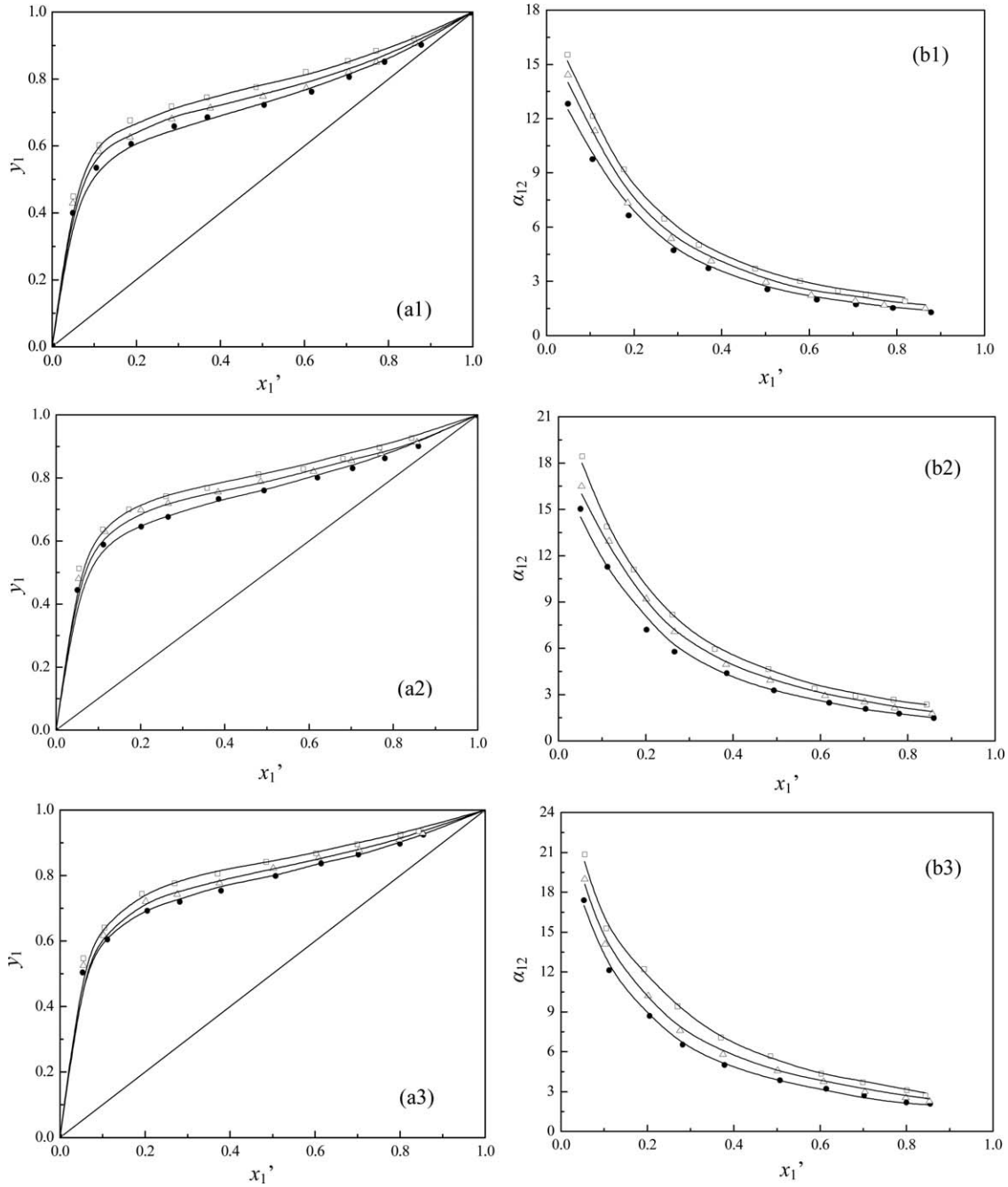


**Figure 2. Isobaric VLE data (a) and relative volatility (b) for the ethanol (1) + water (2) + mixed entrainers ([EMIM]$^+$[Ac]$^-$ (3) + KAc (4)) system at 101.3 kPa.**

**(a1) (b1): $x_{entrainer} = 5\%$ (mole fraction); (a2) (b2): $x_{entrainer} = 10\%$ (mole fraction); (a3) (b3): $x_{entrainer} = 15\%$ (mole fraction). Scattered points, the experimental data; solid lines, the correlated results using the NRTL model. (•) $w_4 = 0$; (▲) $w_4 = 0.02$; (□) $w_4 = 0.05$.**

a weak hydrogen bond donator and acceptor ability, but it can combine with water through hydrogen bonds.

From Figure 4a, one can see that the peaks of these concerned anions lie in the right zone ($\sigma > 0.0082$ e/Å$^2$) and far away from 0.0082 e/Å$^2$, indicating that these anions have strong hydrogen bond acceptor abilities. Thus, the anions can form hydrogen bonds with water (as hydrogen bond donators) and break the interaction between ethanol and water molecules. Meanwhile, the hydrogen bond acceptor ability follows the order of $Ac^- > HCO_3^- \approx Cl^- > NO_3^- > SCN^-$, which is consistent with the selectivity trend of ethanol to water, as shown in Figure 1. Moreover, the $[Ac]^-$ anion has the strongest hydrogen bond acceptor ability, which may play a predominant role in improving the relative volatility of ethanol to water via forming hydrogen bonds with water.

In addition, the $\sigma$-profiles for the cations ($K^+$, $Na^+$, and $[EMIM]^+$) are shown in Figure 4b. It can be observed that the peaks of $Na^+$ and $K^+$ lie in the left zone ($\sigma < -0.0082$ e/Å$^2$) and far away from $-0.0082$, whereas for $[EMIM]^+$, the peaks mainly lie in the range of $-0.0082$ e/Å$^2 < \sigma < 0.0082$ e/Å$^2$, showing that $K^+$ and $Na^+$ have stronger hydrogen bond donator ability than $[EMIM]^+$. Thus, the cations ($Na^+$ and $K^+$), as hydrogen bond donators, can also form hydrogen bonds with water molecules (as

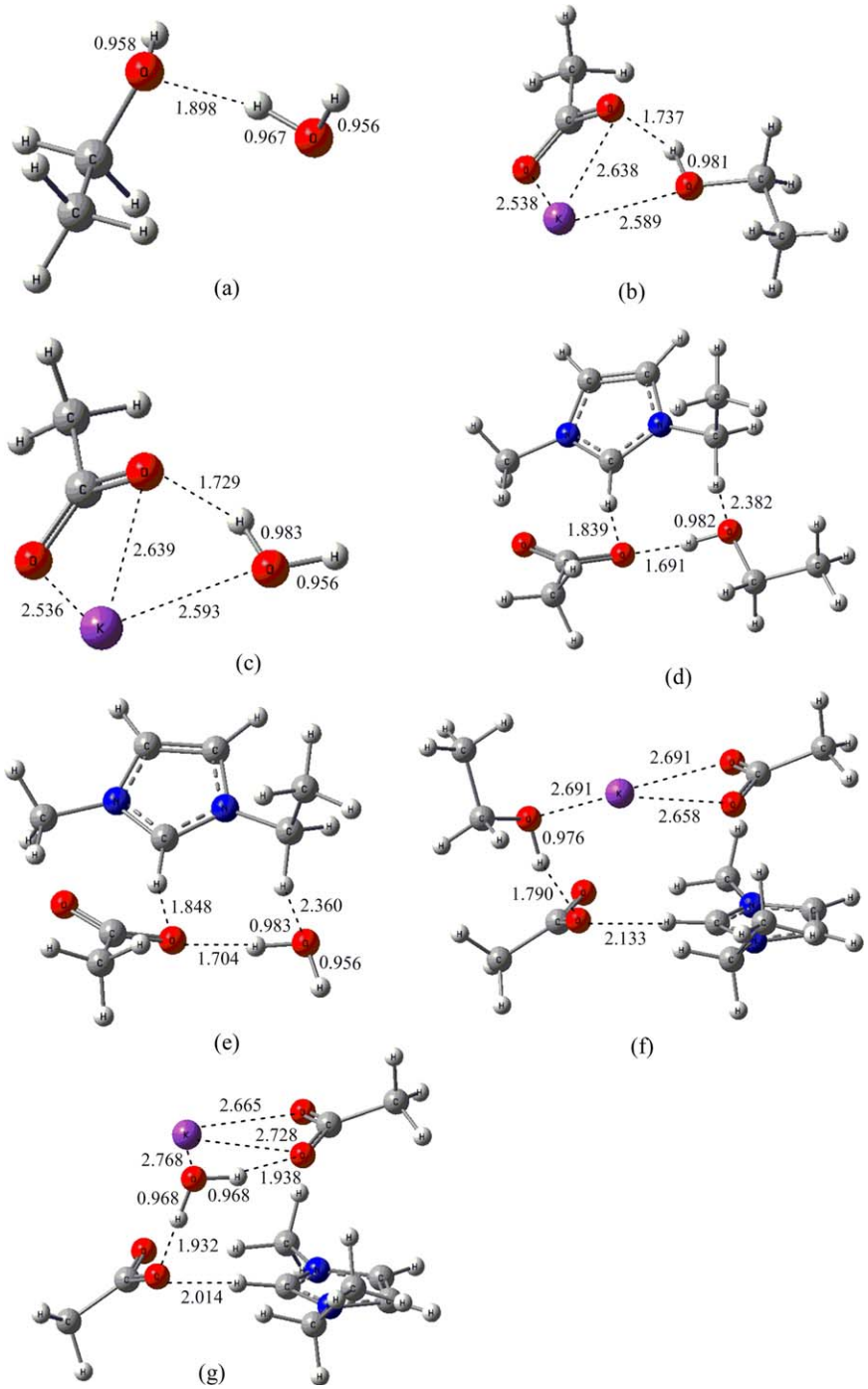


**Figure 3. Optimized geometric structures of (a) ethanol + water, (b) ethanol + KAc, (c) water + KAc, (d) ethanol + $[EMIM]^+[Ac]^-$, (e) water + $[EMIM]^+[Ac]^-$, (f) ethanol + $[EMIM]^+[Ac]^-$ + KAc, and (g) water + $[EMIM]^+[Ac]^-$ + KAc.**

**[Color figure can be viewed in the online issue, which is available at wileyonlinelibrary.com.]**

hydrogen bond acceptor) and weaken the interaction between ethanol and water molecules. The water molecule has the dual ability of being a hydrogen bond acceptor and donator.

**Table 1. Binding Energies Between Entrainer and Water (or Ethanol)**

| Entrainers | Ethanol (kJ $mol^{-1}$) | Water (kJ $mol^{-1}$) |
|---|---|---|
| KAc | −75.6 | −77.0 |
| $[EMIM]^+[Ac]^-$ | −60.6 | −62.1 |
| $[EMIM]^+[Ac]^-$ + KAc | −58.8 | −67.4 |

Thus, the stronger hydrogen bonds with the inorganic solid salts NaAc or KAc with respect to $[EMIM]^+[Ac]^-$ result in the enhancement of relative volatility of ethanol to water. Note that $[EMIM]_1^+$, $[EMIM]_2^+$, and $[EMIM]_3^+$ are the isomers of the $[EMIM]^+$ cation.

*Analysis of the Excess Enthalpy.* The excess enthalpy of solute-IL mixtures as an important thermodynamic quantity can be used to evaluate the nonideality of a solution and analyze the VLE results. For the systems investigated in this work, the interaction between molecules mainly consists of

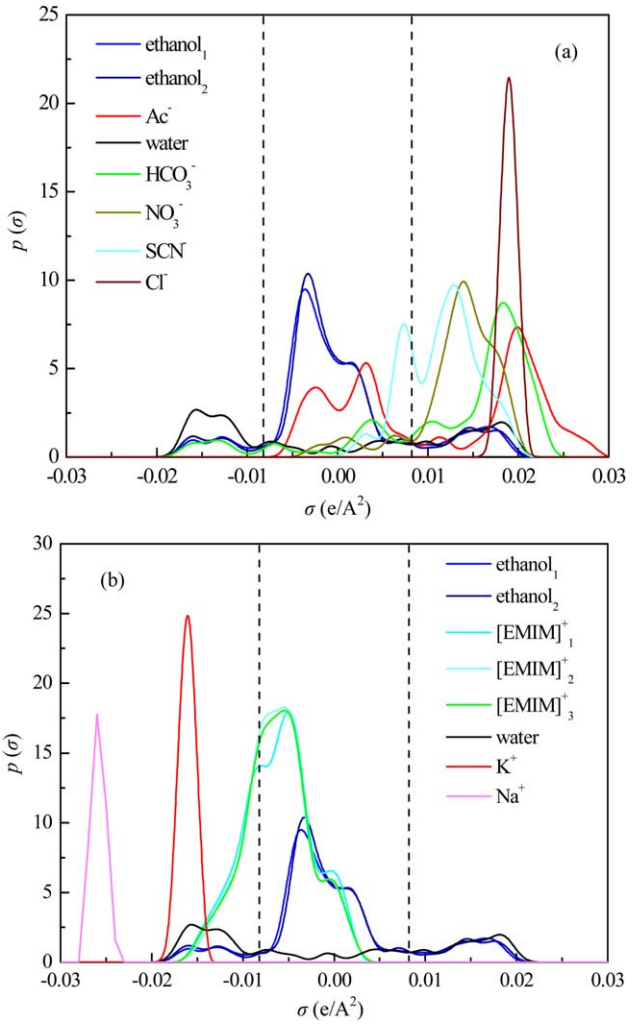


**Figure 4. $\sigma$-profiles for water, ethanol, cations, and anions.**

**[Color figure can be viewed in the online issue, which is available at wileyonlinelibrary.com.]**

electrostatic (misfit), hydrogen bonding (H-bond), and van der Waals (vdW) interactions. Thus, the excess enthalpy ($H^E$) can be expressed by the sum of these contributions

$$H^E = H^E(\text{misfit}) + H^E(\text{H-bond}) + H^E(\text{vdW}) \quad (5)$$

In this work, the excess enthalpies for various water + entrainer (including IL and the mixture of IL and solid inorganic salt) systems, as well as ethanol + entrainer systems, were calculated by the COSMO-RS model.[88] As shown in Figure 5, it is evident that the main part of the excess enthalpy in the investigated systems is the hydrogen bond interaction $H^E$ (H-bond), which is consistent with the $\sigma$-profile analysis as aforementioned. The electrostatic interaction $H^E$ (misfit) is the second contribution to the mixing enthalpy, whereas the van der Waals interaction $H^E$ (vdW) has negligible contribution to the mixing enthalpy.

In all cases, the excess enthalpies of water + entrainer are larger than those of ethanol + entrainer, indicating that the interaction between water and entrainer is stronger than that between ethanol and entrainer. The mixing enthalpies between water and entrainer follow the order: $[EMIM]^+[Ac]^- + KAc > [EMIM]^+[Ac]^- + NaAc > [EMIM]^+[Ac]^- + KHCO_3 > [EMIM]^+[Ac]^- + KNO_3 > [EMIM]^+[Ac]^- + NaNO_3 > [EMIM]^+[Ac]^-$, which is consistent with the selectivity trend of ethanol to water, as shown in Figure 1. This confirms that a higher selectivity is associated with a higher mixing enthalpy of the mixture predicted by the COSMO-RS model.

### *Phase equilibrium model parameters*

The NRTL model parameters ($\Delta g_{ij}$ and $\Delta g_{ji}$) fitted to the experimental data of the ternary and quaternary systems are listed in Table 2. In this case, the average relative deviation (ARD) of the activity coefficients is 7.23% for the ternary system and 6.95% for the quaternary system. For comparison, the results calculated by NRTL are also illustrated in Figure 2, indicating its high accuracy. The isobaric VLE data and the corresponding model parameters are important for the process simulation and design of extractive distillation.

### *Conceptual process design*

In principle, the flow sheet of extractive distillation processes with the single $[EMIM]^+[Ac]^-$ as entrainer is the same as with the mixture of $[EMIM]^+[Ac]^-$ and KAc as entrainers, consisting of an extractive distillation column (EDC) and a entrainer recovery equipment. Considering the entrainer recovery technology, it has been demonstrated that a set of different methods, containing a stripping column with a hot gas ($N_2$ or ethylbenzene), supercritical $CO_2$ extraction, distillation by adding a cosolvent, and evaporation, have been proposed and

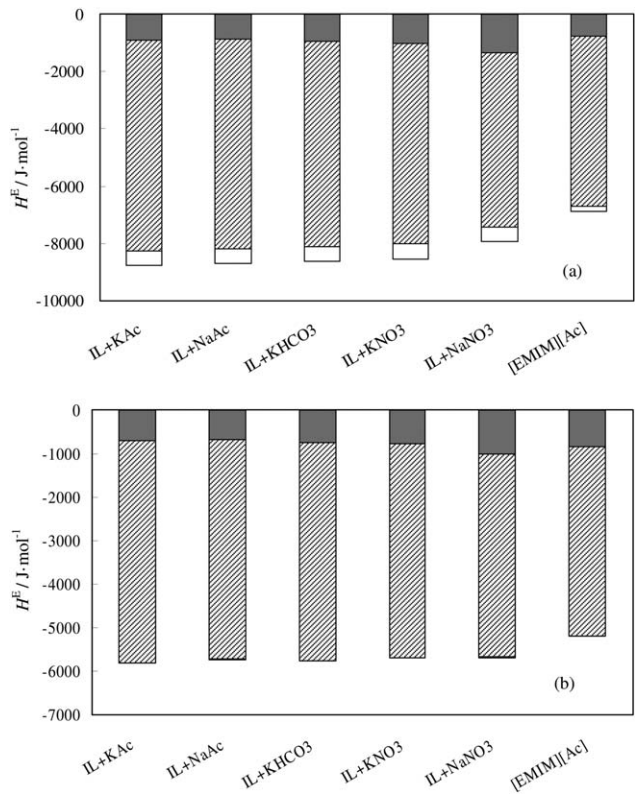


**Figure 5. Excess enthalpies of water (1) + entrainer (2) and ethanol (1) + entrainer (2) systems at $x_1 = 0.9$ and $T = 298.15$ K.**

**(a) water (1) + entrainer (2); (b) ethanol (1) + entrainer (2). IL represents $[EMIM]^+[Ac]^-$, and the mass fraction of solid inorganic salt is kept at 0.05 in the mixed entrainers. (▨) $H^E$ (H-bond); (■) $H^E$ (misfit); (□) $H^E$(vdW).**

**Table 2. Estimated Values of the Binary Parameters in the NRTL Model**

| Component $i$ | Component $j$ | $\alpha_{ij}$ | $\Delta g_{ij}$/J mol$^{-1}$ | $\Delta g_{ji}$/J mol$^{-1}$ |
|---|---|---|---|---|
| Ethanol (1) | Water (2) | 0.40 | $-2216.0 + 6.7055\ T$ | $3698.8 + 4.2758\ T$ |
| Ethanol (1) | [EMIM]$^+$[Ac]$^-$ (3) | 0.30 | −4282.64 | −2775.43 |
| Ethanol (1) | KAc (4) | 0.30 | −3787.51 | −899.80 |
| Water (2) | [EMIM]$^+$[Ac]$^-$ (3) | 0.30 | −3449.16 | −7003.56 |
| Water (2) | KAc (4) | 0.30 | −3698.69 | −7386.17 |
| [EMIM]$^+$[Ac]$^-$ (3) | KAc (4) | 0.47 | −75.94 | −66.11 |

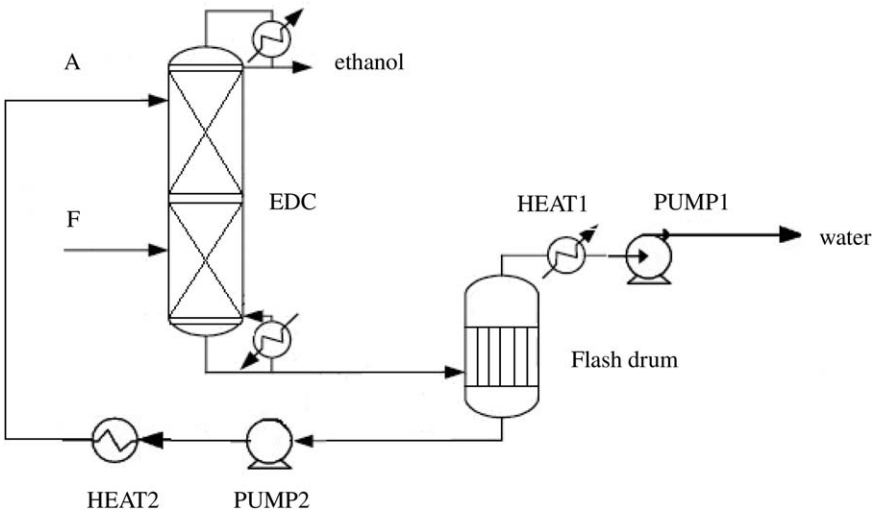


**Figure 6. Extractive distillation process for the separation of ethanol and water with the new mixed entrainers.**

**F and A represent the feed stream and entrainer stream, respectively.**

evaluated for regenerating ILs. Among others, evaporation at low pressures and solvent stripping are the most promising technologies due to their high recovery ability and easy operation.[89] However, the recovery with a flash drum is the simplest and thus was selected as the entrainer recovery method in this work. It is noted that care should be taken during the operation due to the low operating pressure (approximately 15 mbar). The flow sheet of the extractive distillation process with the new mixed entrainers is shown in Figure 6. The feed (ethanol and water mixture) enters into EDC at the middle

**Table 3. Optimized Specifications and Operating Conditions for the Separation of Ethanol and Water Using Different Entrainers**

| | | Entrainers | |
|---|---|---|---|
| Contents | | [EMIM]$^+$[AC]$^-$ | [EMIM]$^+$[AC]$^-$ + KAc |
| Columns | Extractive distillation column (EDC) | | |
| | Pressure (atm) | 1.0 | 1.0 |
| | Total stages | 30 | 30 |
| | Feed stage | 23 | 23 |
| | Entrainer feed stage | 3 | 3 |
| | Mass reflux ratio | 1.1 | 1.1 |
| | Distillate rate (kg·h$^{-1}$) | 80 | 80 |
| | Flash drum | | |
| | Temperature (°C) | 160 | 160 |
| | Pressure (atm) | 0.015 | 0.013 |
| Streams | Feed stream | | |
| | Temperature (°C) | 78 | 78 |
| | Pressure (atm) | 1.0 | 1.0 |
| | Component flow rate (kg·h$^{-1}$) | | |
| | Ethanol | 80 | 80 |
| | Water | 20 | 20 |
| | Entrainer stream | | |
| | Temperature (°C) | 78 | 78 |
| | Pressure (atm) | 1.0 | 1.0 |
| | Component flowrate (kg·h$^{-1}$) | | |
| | [EMIM]$^+$[Ac]$^-$ | 100 | 85 |
| | KAc | 0 | 1 |

Table 4. Comparison of the Process Simulation Results Between Mixed Entrainers and the Benchmark Solvent

| Contents | | | Entrainers | |
|---|---|---|---|---|
| | | | $[EMIM]^+[AC]^-$ | $[EMIM]^+[AC]^-$ + KAc |
| Streams | Distillate stream | Temperature (°C) | 78.35 | 78.35 |
| | | Ethanol product purity (mass fraction) | 1.000 | 0.999 |
| | Bottom stream of EDC | Temperature (°C) | 132.25 | 127.75 |
| | | Composition (mass fraction) | | |
| | | Ethanol | trace | trace |
| | | Water | 0.167 | 0.188 |
| | | $[EMIM]^+[Ac]^-$ | 0.833 | 0.802 |
| | | KAc | – | 0.009 |
| | Top stream of flash drum | Temperature (°C) | 160 | 160 |
| | | Mass flowrate ($kg \cdot h^{-1}$) | 19.51 | 19.62 |
| | | Water content (mass fraction) | 0.998 | 0.995 |
| | Recycled entrainer stream | Temperature (°C) | 160 | 160 |
| | | Mass flowrate ($kg \cdot h^{-1}$) | 100.49 | 86.38 |
| | | Composition (mass fraction) | | |
| | | Water | 0.005 | 0.005 |
| | | $[EMIM]^+[Ac]^-$ | 0.995 | 0.984 |
| | | KAc | – | 0.012 |
| Heat duty | EDC | Condenser (kW) | −39.44 | −39.49 |
| | | Reboiler (kW) | 49.89 | 40.87 |
| | Flash drum | Heat duty (kW) | 19.48 | 15.29 |
| | Total heat duty (kW) | | 69.37 | 56.16 |
| | Heat exchanger 1 (HEAT1) | Temperature of outlet (°C) | 13.25 | 10.85 |
| | | Heat duty (kW) | −14.81 | −14.91 |
| | Heat exchanger 2 (HEAT2) | Inlet Temperature (°C) | 160 | 160 |
| | | Outlet temperature (°C) | 78 | 78 |
| | | Heat duty (kW) | −16.77 | −3.43 |

stage, whereas the entrainer is introduced at the top. Then, the anhydrous ethanol is produced after total condensation at the top of the EDC. The entrainer at the bottom containing some water is introduced into the flash drum, which operates under vacuum condition, to remove water from the entrainer. The dried entrainer is recycled back to the top of the EDC after cooling.

The optimized specifications were determined using the Design Specs module and sensitivity analysis in Aspen Plus with the following constraints: (a) mass purity $> 99.9\%$ for ethanol at the top of the EDC; (b) mass purity $> 99.4\%$ for water at the top of the flash drum; and (c) the mass fraction of water in the entrainer at the bottom of the flash drum less than 0.5%, which ensures a high purity of ethanol product obtained at the top of EDC. The operating conditions and optimized specifications are listed in Table 3.

The comparison of the simulation results between mixed entrainers and the benchmark solvent is given in Table 4. We can see that the recycled flow rate of entrainers in the two processes decreases from 100.49 kg $h^{-1}$ for the single $[EMIM]^+[Ac]^-$ to 86.38 kg $h^{-1}$ for the mixture of $[EMIM]^+[Ac]^-$ and KAc. Conversely, the total heat duty, defined as the addition of the reboiler heat duties of the EDC and the flash drum, decreases 19.04% when using the mixed entrainers. That is to say, the new mixed entrainers are more promising for saving energy and IL consumption.

## Conclusions

To the best of our knowledge, this is the first work to propose the mixture of IL and solid inorganic salt as a new type of entrainer in extractive distillation. Both the VLE experiments and the COSMO-RS calculations showed that it is an effective way to increase the relative volatility of ethanol to water by adding a small amount of solid inorganic salt into the benchmark IL $[EMIM]^+[Ac]^-$. Moreover, the mixture of $[EMIM]^+[Ac]^-$ and KAc was suggested as having the most potential among all the entrainers investigated.

We looked for some theoretical insights at the molecular level by analyzing the binding energy, $\sigma$-profile, and the mixing enthalpy by means of DFT and the COSMO-RS model. The strong interaction between the new entrainer and water molecules weakens the ethanol–water interactions, thus increasing the relative volatility of ethanol to water. The results from the experiments (by VLE measurement) and the theoretical analysis (by the combination of DFT and COSMO-RS model) are consistent. In this sense, the COSMO-RS model can be used not only for entrainer screening in separation science but also for providing deeper theoretical insight into the selectivity behavior.

Based on the experimentally measured VLE data, the EQ stage model RadFrac was used to simulate the conceptual process design. It was found that the new entrainer was indeed more promising in saving energy and entrainer consumption. In comparison with the benchmark IL $[EMIM]^+[Ac]^-$, the ratio of entrainer to feed decreases 14.04%, and the overall heat duties on the reboilers decreases 19.04%.

It is worth mentioning that when using the new entrainers, there is no additional streams and equipments required based on the current state of the art of extractive distillation processes using single ILs as entrainers. In other words, the strategy of IL intensification presented in this work is easily implemented in practice only by replacing entrainer, and it can be directly extended to the separation of other systems by extractive distillation with ILs.

## Acknowledgment

This work was financially supported by the National Nature Science Foundation of China under Grants (Nos. 21121064 and 21076008).

## Literature Cited


1. Barba D, Brandani V, Giacomo GD. Hyperazeotropic ethanol salted-out by extractive distillation. Theoretical evaluation and experimental check. *Chem Eng Sci*. 1985;40:2287–2292.
2. Furter WF. Extractive distillation by salt effect. *Chem Eng Commun*. 1992;116:35–40.
3. Furter WF. Production of fuel-grade ethanol by extractive distillation employing the salt effect. *Sep Purif Methods*. 1993;22:1–21.
4. Lei Z, Zhou R, Duan Z. Application of scaled particle theory in extractive distillation with salt. *Fluid Phase Equilib*. 2002;200:187–201.
5. Berg L. Selecting the agent for distillation processes. *Chem Eng Prog*. 1969;65:52–57.
6. Berg L. Separation of benzene and toluene from close boiling nonaromatics by extractive distillation. *AIChE J*. 1983;29:961–966.
7. Chen B, Lei Z, Li J. Separation on aromatics and nonaromatics by extractive distillation with NMP. *J Chem Eng Jpn*. 2003;36:20–24.
8. Gil ID, Gómez JM, Rodríguez G. Control of an extractive distillation process to dehydrate ethanol using glycerol as entrainer. *Comput Chem Eng*. 2012;39:129–142.
9. Lei Z, Wang H, Zhou R, Duan Z. Influence of salt added to solvent on extractive distillation. *Chem Eng J*. 2002;87:149–156.
10. Lei Z, Wang H, Zhou R, Duan Z. Solvent improvement for separating C4 with ACN. *Comput Chem Eng*. 2002;26:1213–1221.
11. Lei Z, Wang H, Zhou R, Duan Z. Process improvement on separating C4 by extractive distillation. *Chem Eng J*. 2002;87:379–386.
12. Gil ID, Uyazán AM, Aguilar JL, Rodríguez G, Caicedo LA. Separation of ethanol and water by extractive distillation with salt and solvent as entrainer: process simulation. Brazilian. *J Chem Eng*. 2008; 25:207–215.
13. Seiler M, Jork C, Kavarnou A, Arlt W, Hirsch R. Separation of azeotropic mixtures using hyperbranched polymers or ionic liquids. *AIChE J*. 2004;50:2439–2454.
14. Jork C, Seiler M, Beste YA, Arlt W. Influence of ionic liquids on the phase behavior of aqueous azeotropic systems. *J Chem Eng Data*. 2004;49:852–857.
15. Dietz ML. Ionic liquids as extraction solvents: where do we stand? *Sep Sci Technol*. 2006;41:2047–2063.
16. Sun X, Luo H, Dai S. Ionic liquids-based extraction: a promising strategy for the advanced nuclear fuel cycle. *Chem Rev*. 2012;112: 2100–2128.
17. Marciniak A. Influence of cation and anion structure of the ionic liquid on extraction processes based on activity coefficients at infinite dilution. A review. *Fluid Phase Equilib*. 2010;294:213–233.
18. Poole CF, Poole SK. Extraction of organic compounds with room temperature ionic liquids. *J Chromatogr A*. 2010;1217:2268–2286.
19. Pereiro AB, Rodríguez A. Applications of ionic liquids in azeotropic mixtures separation. In: Kokorin A, editor. *Ionic Liquids: Applications and Perspectives*, Rijeka, Croatia: InTech, 2011:225–242.
20. Pereiro AB, Araújo JMM, Esperança JMSS, Marrucho IM, Rebelo LPN. Ionic liquids in separations of azeotropic systems-a review. *J Chem Thermodyn*. 2012;46:2–28.
21. Meindersma GW, Quijada-Maldonado E, Aelmans TAM, Hernandez JPG, de Haan AB. Ionic liquid in extractive disillation of ethanol/water: from laboratory to pilot plant. In: Visser AE, Bridges NJ, Rogers RD, editors. *Ionic Liquids: Science and Applications*, Washington, DC: American Chemical Society, ACS Symposium Series, 2012:239–257.
22. Jork C, Kristen C, Pieraccini D, Stark A, Chiappe C, Beste YA, Arlt W. Tailor-made ionic liquids. *J Chem Thermodyn*. 2005;37:537–558.
23. Welton T. Room-temperature ionic liquids. Solvents for synthesis and catalysts. *Chem Rev*. 1999;99:2071–2083.
24. Brennecke JF, Maginn EJ. Ionic liquids: innovative fluids for chemical processing. *AIChE J*. 2001;47:2384–2389.
25. Baker GA, Banker SN, Pandey S, Bright FV. An analytical view of ionic liquids. *Analyst*. 2005;130:800–808.
26. Han XX, Armstrong DW. Ionic liquids in separations. *Acc Chem Res*. 2007;40:1079–1086.
27. Marsh KN, Boxall JA, Lichtenthaler R. Room temperature ionic liquids and their mixtures—a review. *Fluid Phase Equilib*. 2004; 219:93–98.
28. Dong Q, Muzny CD, Kazakov A, Diky V, Magee JW, Widegren JA, Chirico RD, Marsh KN, Frenkel M. IL thermo: a free-access web database for thermodynamic properties of ionic liquids. *J Chem Eng Data*. 2007;52:1151–1159.
29. Seddon, KR. Ionic liquids for clean technology. *J Chem Technol Biotechnol*. 1997;68:351–356.
30. Lei Z, Chen B, Li C. COSMO-RS modeling on the extraction of stimulant drugs from urine sample by the double actions of supercritical carbon dioxide and ionic liquid. *Chem Eng Sci*. 2007;62: 3940–3950.
31. Lei Z, Arlt W, Wasserscheid P. Separation of 1-hexene and n-hexane with ionic liquids. *Fluid Phase Equilib*. 2006;241:290–299.
32. Lei Z, Arlt W, Wasserscheid P. Selection of entrainers in the 1-hexene/n-hexane system with a limited solubility. *Fluid Phase Equilib*. 2007;260:29–35.
33. Momoh SO. Assessing the accuracy of selectivity as a basis for solvent screening in extractive distillation processes. *Sep Sci Technol*. 1991;26:729–742.
34. Calvar N, González B, Gómez E, Domínguez Á. Vapor-liquid equilibria for the ternary system ethanol + water + 1-butyl-3-methylimidazolium chloride and the corresponding binary systems at 101.3 kPa. *J Chem Eng Data*. 2006;51:2178–2181.
35. Calvar N, González B, Gómez E, Domínguez Á. Study of the behaviour of the azeotropic mixture ethanol-water with imidazolium-based ionic liquids. *Fluid Phase Equilib*. 2007;259:51–56.
36. Calvar N, González B, Gómez E, Domínguez Á. Vapor-liquid equilibria for the ternary system ethanol + water + 1-ethyl-3-methylimidazolium ethylsulfate and the corresponding binary systems containing the ionic liquid at 101.3 kPa. *J Chem Eng Data*. 2008;53:820–825.
37. Calvar N, González B, Gómez E, Domínguez Á. Vapour-liquid equilibria for the ternary system ethanol + water + 1-butyl-3-methylimidazolium methylsulfate and the corresponding binary systems at 101.3 kPa. *J Chem Eng Data*. 2009;54:1004–1008.
38. Calvar N, Gómez E, González B, Domínguez Á. Experimental vapor−liquid equilibria for the ternary system ethanol + water + 1-ethyl-3-methylpyridinium ethylsulfate and the corresponding binary systems at 101.3 kPa: study of the effect of the cation. *J Chem Eng Data*. 2010;55:2786–2791.
39. Orchillés AV, Miguel PJ, Vercher E, Martínez-Andreu A. Using 1-ethyl-3-methylimidazolium trifluoromethanesulfonate as an entrainer for the extractive distillation of ethanol + water mixtures. *J Chem Eng Data*. 2010;55:1669–1674.
40. Orchillés AV, Miguel PJ, Llopis FJ, Vercher E, Martínez-Andreu A. Isobaric vapor−liquid equilibria for the extractive distillation of ethanol + water mixtures using 1-ethyl-3-methylimidazolium dicyanamide. *J Chem Eng Data*. 2011;56:4875–4880.
41. Ge Y, Zhang L, Yuan X, Geng W, Ji J. Selection of ionic liquids as entrainers for separation of (water and ethanol). *J Chem Thermodyn*. 2008;40:1248–1252.
42. Li Q, Zhang J, Lei Z, Zhu J. Zhu J, Huang X. Selection of ionic liquids as entrainers for the separation of ethyl acetate and ethanol. *Ind Eng Chem Res*. 2009;48:9006–9012.
43. Li Q, Xing F, Lei Z, Wang B, Chang Q. Isobaric vapor−liquid equilibrium for isopropanol + water + 1-ethyl-3-methylimidazolium tetrafluoroborate. *J Chem Eng Data*. 2008;53:275–279.
44. Li Q, Zhang J, Lei Z, Zhu J, Xing F. Isobaric vapor−liquid equilibrium for ethyl acetate + ethanol + 1-ethyl-3-methylimidazolium tetrafluoroborate. *J Chem Eng Data*. 2009;54:193–197.
45. Li Q, Zhu W, Wang H, Ran X, Fu Y, Wang B. Isobaric vapor−liquid equilibrium for the ethanol + water + 1,3-dimethylimidazolium dimethylphosphate system at 101.3 kPa. *J Chem Eng Data*. 2012;57: 696–700.
46. Kamihama N, Matsuda H, Kurihara K, Tochigi K, Oba S. Isobaric vapor−liquid equilibria for ethanol + water + ethylene glycol and its constituent three binary systems. *J Chem Eng Data*. 2012;57:339–344.
47. Herington EFG. Tests for the consistency of experimental isobaric vapor–liquid equilibrium data. *J Inst Petrol*. 1951;37:457–470.
48. Gill BK, Rattan VK, Kapoor S. Experimental isobaric vapor–liquid equilibrium data for binary mixtures of cyclic ethers with (1-methylethyl)benzene. *J Chem Eng Data*. 2008;53:2041–2043.
49. Yang SK, Zhang YP, Wang XJ, Qiao MY, Zhu Y. Isobaric VLE data for 1-methyl-3-ethylbenzene or 1-methyl-4-ethylbenzene + 1,2,4-trimethylbenzene at 20 kPa. *J Chem Thermodyn*. 2013;60:52–56.
50. Frisch MJ, Trucks GW, Schlegel HB, Scuseria GE, Robb MA, Cheeseman JR, Montgomery JA, Vreven T, Kudin KN, Burant JC, Millam JM, Iyengar SS, Tomasi J, Barone V, Mennucci B, Cossi M, Scalmani G, Rega N, Petersson GA, Nakatsuji H, Hada M, Ehara M, Toyota K, Fukuda R, Hasegawa J, Ishida M, Nakajima T, Honda Y, Kitao O, Nakai H, Klene M, Li X, Knox JE, Hratchian HP, Cross JB, Bakken V, Adamo C, Jaramillo J, Gomperts R, Stratmann RE, Yazyev O, Austin AJ, Cammi R, Pomelli C, Ochterski JW, Ayala PY, Morokuma K, Voth GA, Salvador P, Dannenberg JJ, Zakrzewski VG, Dapprich S, Daniels AD, Strain MC, Farkas O,

Malick DK, Rabuck AD, Raghavachari K, Foresman JB, Ortiz JV, Cui Q, Baboul AG, Clifford S, Cioslowski J, Stefanov BB, Liu G, Liashenko A, Piskorz P, Komaromi I, Martin RL, Fox DJ, Keith T, Al-Laham MA, Peng CY, Nanayakkara A, Challacombe M, Gill PMW, Johnson B, Chen W, Wong MW, Gonzalez C, Pople JA. *Gaussian 03, Revision B.05*. Wallingford, CT: Gaussian, Inc., 2004.
51. Gao T, Andino JM, Raul Alvarez-Idaboy J. Computational and experimental study of the interactions between ionic liquids and volatile organic compounds. *Phys Chem Chem Phys*. 2010;12:9830–9838.
52. Ruiz E, Ferro VR, Palomar J, Ortega J, Rodriguez JJ. Interactions of ionic liquids and acetone: thermodynamic properties, quantum-chemical calculations, and NMR analysis. *J Phys Chem B*. 2013; 117:7388–7398.
53. Zhao Y, Schultz NE, Truhlar DG. Design of density functionals by combining the method of constraint satisfaction with parametrization for thermochemistry, thermochemical kinetics, and noncovalent interactions. *J Chem Theory Comput*. 2006;2:364–382.
54. Klamt A. Conductor-like screening model for real solvents: a new approach to the quantitative calculation of solvation phenomena. *J Phys Chem*. 1995;99:2224–2235.
55. Klamt A, Jonas V, Burger T, Lohrenz JC. Refinement and parametrization of COSMO-RS. *J Phys Chem A*. 1998;102:5074–5085.
56. Klamt A, Eckert F. COSMO-RS: a novel and efficient method for the a priori prediction of thermophysical data of liquids. *Fluid Phase Equilib*. 2000;172:43–72.
57. Eckert F, Klamt A. Fast solvent screening via quantum chemistry: COSMO-RS approach. *AIChE J*. 2002;48:369–385.
58. Li Q, Zhang J, Lei Z, Zhu J, Wang B, Huang X. Isobaric vapor–liquid equilibrium for (propan-2-ol + water + 1-ethyl-3-methylimidazolium tetrafluoroborate. *J Chem Eng Data*. 2009;54:2785–2788.
59. Orchillés AV, Miguel PJ, González-Alfaro V, Vercher E, Martínez-Andreu A. Isobaric vapor–liquid equilibria of 1-propanol + water + trifluoromethanesulfonate-based ionic liquid ternary systems at 100 kPa. *J Chem Eng Data*. 2011;56:4454–4460.
60. Li Q, Zhu W, Fu Y, Wang H, Li L, Wang B. Isobaric vapor–liquid equilibrium for methanol + dimethyl carbonate + 1-octyl-3-methylimidazolium tetrafluoroborate. *J Chem Eng Data*. 2012;57: 1602–1606.
61. Jongmans M, Raijmakers M, Schuur B, Haan A. Binary and ternary vapor−liquid equilibrium data of the system (ethylbenzene + styrene + 4-methyl-N-butylpyridinium tetrafluoroborate) at vacuum conditions and liquid−liquid equilibrium data of their binary systems. *J Chem Eng Data*. 2012;57:626–633.
62. Zhang L, Han J, Deng D, Ji J. Selection of ionic liquids as entrainers for separation of water and 2-propanol. *Fluid Phase Equilib*. 2007; 255:179–185.
63. Cai F, Wu X, Chen C, Chen X, Asumana C, Haque MR, Yu G. Isobaric vapor–liquid equilibrium for methanol + dimethyl carbonate + phosphoric-based ionic liquids. *Fluid Phase Equilib*. 2013;352: 47–53.
64. Hwang IC, Kwon RH, Park SJ. Azeotrope breaking for the system ethyl tert-butyl ether (ETBE) + ethanol at 313.15 K and excess properties at 298.15 K for mixtures of ETBE and ethanol with phosphonium-based ionic liquids. *Fluid Phase Equilib*. 2013;344: 32–37.
65. Tian Z, Cui X, Cai J, Zhang Y, Feng T, Peng Y, Xue L. Isobaric VLE data for the system of butan-1-ol + butyl ethanoate + 1-butyl-3-methylimidazolium bis[(trifluoromethyl)sulfonyl]imide. *Fluid Phase Equilib*. 2013;352:75–79.
66. Andreatta AE, Arce A, Rodil E, Soto A. Physical properties and phase equilibria of the system isopropyl acetate + isopropanol + 1-octyl-3-methyl-imidazolium bis(trifluoromethylsulfonyl)imide. *Fluid Phase Equilib*. 2010;287:84–94.
67. Press WH, Flannery BP, Teukolsky SA, Vetterling WT. *Numerical Recipes in FORTRAN: The Art of Scientific Computing*, 2nd ed. Cambridge, UK: Cambridge University Press, 1992.
68. Tang Y, Huang H, Chien I. Design of a complete ethyl acetate reactive distillation system. *J Chem Eng Jpn*. 2003;36:1352–1363.
69. Valderrama JO, Rojas RE. Critical properties of ionic liquids. *Revisited*. *Ind Eng Chem Res*. 2009;48:6890–6900.
70. Valderrama JO, Zarricueta K. A simple and generalized model for predicting the density of ionic liquids. *Fluid Phase Equilib*. 2009; 275:145–154.
71. Remesh LG, Coutinho JAP. A group contribution method for heat capacity estimation of ionic liquid. *Ind Eng Chem Res*. 2008;47: 5751–5757.
72. Palomar J, Ferro VR, Torrecilla JS, Rodriguez F. Density and molar volume predictions using COSMO-RS for ionic liquids. An approach to solvent design. *Ind Eng Chem Res*. 2007;46:6041–6048.
73. Palomar J, Torrecilla JS, Ferro VR, Rodriguez F. Development of an a priori ionic liquid design tool. 1. Integration of a novel COSMO-RS molecular descriptor on neural networks. *Ind Eng Chem Res*. 2008;47:4523–4532.
74. Palomar J, Torrecilla JS, Ferro VR, Rodriguez F. Development of a priori ionic liquid design tool. 2. Ionic liquid selection through the prediction of COSMO-RS molecular descriptor by inverse neural network. *Ind Eng Chem Res*. 2009;48:2257–2265.
75. Bulut S, Eiden P, Beichel W, Slattery JM, Beyersdorff TF, Schubert TJS, Krossing I. Temperature dependence of the viscosity and conductivity of mildly functionalized and non-functionalized Tf2N (-) ionic liquids. *Chem Phys Chem*. 2011;12:2296–2310.
76. Eiden P, Bulut S, Koechner T, Friedrich C, Schubert T, Krossing I. In silico predictions of the temperature-dependent viscosities and electrical conductivities of functionalized and nonfunctionalized ionic liquids. *J Phys Chem B*. 2011;115:300–309.
77. Diedenhofen M, Klamt A, Marsh K, Schaefer A. Prediction of the vapor pressure and vaporization enthalpy of 1-n-alkyl-3-methylimidazolium-bis-(trifluoromethanesulfonyl) amide ionic liquids. *Phys Chem Chem Phys*. 2007;9:4653–4656.
78. Diedenhofen M, Klamt A. COSMO-RS as a tool for property prediction of IL mixtures-a review. *Fluid Phase Equilib*. 2010;294:31–38.
79. Ferro VR, Ruiz E, Tobajas M, Palomar JF. Integration of COSMO-based methodologies into commercial process simulators: separation and purification of reuterin. *AIChE J*. 2012;58:3404–3415.
80. Ferro VR, Ruiz E, de Riva J, Palomar J. Introducing process simulation in ionic liquids design/selection for separation processes based on operational and economic criteria through the example of their regeneration. *Sep Purif Technol*. 2012;97:195–204.
81. Bedia J, Ruiz E, de Riva J, Ferro VR, Palomar J, Rodriguez JJ. Optimized ionic liquids for toluene absorption. *AIChE J*. 2013;59:1648–1656.
82. Tong JS. *Thermophysical Properties of Fluids*. Beijing: China Petrochemical Press, 1996.
83. Klamt A, Eckert F, Arlt W. COSMO-RS: an alternative to simulation for calculating thermodynamic properties of liquid mixtures. *Annu Rev Chem Biomed Eng*. 2010;1:101–122.
84. Klamt A, Reinisch J, Eckert F, Hellweg A, Diedenhofen M. Polarization charge densities provide a predictive quantification of hydrogen bond energies. *Phys Chem Chem Phys*. 2012;14:955–963.
85. Li J, Yang X, Chen K, Zheng Y, Peng C, Liu H. Sifting ionic liquids as additives for separation of acetonitrile and water azeotropic mixture using the COSMO-RS method. *Ind Eng Chem Res*. 2012;51:9376–9385.
86. Banerjee T, Singh M, Khanna A. Prediction of binary VLE for imidazolium based ionic liquid systems using COSMO-RS. *Ind Eng Chem Res*. 2006;45:3207–3219.
87. Freire M, Santos L, Marrucho IM, Coutinho J. Evaluation of COSMO-RS for the prediction of LLE and VLE of alcohols + ionic liquids. *Fluid Phase Equilib*. 2007;255:167–178.
88. Navas A, Ortega J, Vreekamp R, Marrero E, Palomar J. Experimental thermodynamic properties of 1-butyl-2-methylpyridinium tetrafluoroborate [b2mpy][BF4] with water and with alkan-1-ol and their interpretation with the COSMO-RS methodology. *Ind Eng Chem Res*. 2009;48:2678–2690.
89. Jongmansa MTG, Trampé J, Schuur B, de Haan AB. Solute recovery from ionic liquids: a conceptual design study for recovery of styrene monomer from [4-mebupy][BF4]. *Chem Eng Process*. 2013;70:148–161.

*Manuscript received Sept. 11, 2013, and revision received Mar. 31, 2014.*